Indonesian Journal of Electrical Engineering and Computer Science
Vol. 40, No. 3, December 2025, pp. 1368~1376
ISSN: 2502-4752, DOI: 10.11591/ijeecs.v40.i3.pp1368-1376

Effective medium ratio obeying metamaterial absorber for 5G sub-7 GHz and sub-8 GHz applications

Mohammad Jakir Hossain, Md. Alim Uddin, Md. Mesbahul Islam, Keya Ghosh, Nusrat Jahan, Mukta Akter Asma
Department of Electrical and Electronic Engineering, Dhaka University of Engineering and Technology (DUET), Gazipur, Bangladesh

Article Info

Article history:

Received Jun 1, 2025
Revised Nov 1, 2025
Accepted Nov 16, 2025

Keywords:

5G communication technology
Effective medium ratio
Miniature metamaterial absorber
Multi-square split-ring resonator

ABSTRACT

Metamaterials possess the capability to enhance fifth-generation (5G) communication technology. This article proposes an innovative construction of a miniature metamaterial absorber (MMA) with a dramatically improved effective medium ratio (EMR) characterized by utilizing a multi-square split-ring resonator (MSSRR) MMA unit cell specifically designed for operation in the 5G sub-7 GHz and Sub-8 GHz frequency bands. The unit cell of the MMA is designed using a commercially available FR-4 material with εr=4.3, which is cost-effective. The proposed MMA achieves a remarkably high EMR of 9.83, indicating superior compactness and design efficiency. The MMA of interest operates with absorbance peaks of 70.632%, 96.936%, and 79.930% within the frequencies of 3.554 GHz, 4.940 GHz, and 8.335 GHz, respectively. Along with the absorption analysis, our examination also includes E-field, H-field, surface current, and power flow. The expected MMA has proven potential for application in some frequency bands related to 5G, released absorption signal, and specific absorption rate (SAR) assistance.

Corresponding Author:

Mohammad Jakir Hossain
Department of Electrical and Electronic Engineering
Dhaka University of Engineering and Technology (DUET)
Gazipur, Bangladesh
Email: jakir@duet.ac.bd

1. INTRODUCTION

Metamaterials are engineered materials that have unique electromagnetic properties. They are used in various applications such as energy harvesting, filtration, sensing, polarization conversion, invisibility cloaks, antenna design, and the creation of photonic devices. Metamaterials have the potential to improve fifth-generation (5G) communication technology and are becoming more common in the manufacturing of 5G devices [1]. Currently, 5G communication is creating new development. The lower frequency bands are widely used for LTE/4G, and the even higher frequency millimeter-wave band is still a hot topic of research. 5G communication [2] will use the midband, the sub-7 GHz spectrum. The FCC opened up new bands for 5G below 7 GHz and this frequency range was reserved and assigned by the Ministry of Industry and Information Technology (MIIT) of the PRC Some B41/N41 frequencies at 2.5/2.6 GHz; 3.7–3.98 GHz; 4.94-4.99 GHz (licensed) All 5.9-7.1 GHz (Unlicensed) B41/N41 at 2.5/2.6 GHz; 3.3-3.6 GHz; 4.8–5 GHz [B1-3] This frequency was some recommended by researchers have been Note 40–100 MHz bandwidth [2]-[4]. Ideal handling is essential for an metamaterial absorber (MMA) in this range. Absorber's overall bands have been developed, or mostly some are not limited to where the absorption reached [5]. Pickle the type of devices in which random energy absorption influences their functions, broadband absorbers using

metamaterials [3], [6]. These absorbers operate at frequencies of 3.2-11 GHz and 2.2-5.83 GHz. The article suggests a broadband MMA at 7.18-8.8 GHz using a broadband sectional resonator [7]. One MMA with a mandarin line was reported to exhibit broadband in the line direction with the working frequency range of 1.84–5.96 GHz [8], also are reported devices having similar expression based on PET substrate working in the bandwidth of 1.0 to 4.5 GHz [9]. Flexible origami-based microwave absorber with tunable absorption bandwidth from 3.4 to 18 GHz. Other patch designs have also been explored [10]-[14]. Yet, bigger sizes pose challenges to composite patch designs as the majority of MMAs operate with FR-4 substrates. Various pattern designs of metal rings have been presented and used for triple absorption bands. Where [12], [13] have utilized a pair of metal rings with copper coating at 3.36, 3.95, and 10.48 GHz and three metallic resonators at 3.95, 5.92, and 9.21 GHz. A double circular o-slot with different metallic resonators at 1.75, 2.17, and 2.6 GHz and six concentric rings at 2.9, 4.18, and 9.25 GHz. The latter circular rings and inner Jerusalem crosses have been verified at 4.4 GHz, 6.05 GHz, and 13.9 GHz [12], [14]. For pure MMAs with high performance and large area characteristics, dual-band MMAs with only two bands are achieved, offering a narrow bandwidth. Notably, there are no dual-band MMAs that closely match this, but they do cover a gap in the sub-6 GHz unlicensed spectrum [15], [16]. Many papers have studied MMA with values ranging from 2 to 9 GHz [3], [6], [10]-[17]. An effective medium ratio (EMR) value of ≥0.43 for statistical significance to allow for smaller MMA structural designs. A polarization-insensitive perfect absorber based on a near-zero index metamaterial (NZIM) with a swastika-shaped resonator on an FR4 substrate achieves near-unity absorption at multiple resonant frequencies across the C, X, and Ku bands [18]. A compact square-shaped metamaterial (SM) on FR-4 is proposed to reduce EM energy absorption in human head tissue from 5G exposure, aiming to minimize specific absorption rate (SAR) and validated through simulations and experiments [19]. Another wide-angle, polarization-insensitive MMA achieves over 90% absorption at seven microwave frequencies, demonstrating strong higher-order electric resonance with simulation and experimental support [20]. It maintains high absorption from 5.2 to 18.1 GHz, stable under oblique incidence for both TE and TM modes [21].

In this study, we have designed an MSSRR MMA for applications within the 5G sub-7 GHz and Sub-8 GHz frequency range. The unit cell is designed using a commercially used FR-4 substrate in the middle and copper (annealed) in the ground and patch with dimensions 8.6 mm×8.6 mm×1.6 mm. At a frequency of 3.554 GHz, the absorption is 70.63%. At 4.940 GHz, the absorption significantly increases to 96.94%, indicating the highest absorption efficiency, and at 8.335 GHz, its absorption is 79.93%.

2. MATERIALS AND METHODS

2.1. Impedance matching and effective medium theory

Impedance matching in metamaterials ensures that the structure's input impedance closely matches the impedance of free space ($Z_0 \approx 377\ \Omega$), minimizing reflection at the interface. When matched, more incident electromagnetic energy enters and is absorbed by the metamaterial, enhancing its performance.

$$Z(\omega) = \sqrt{\frac{\mu_{eff}(\omega)}{\varepsilon_{eff}(\omega}} \quad (1)$$

When $Z(\omega) \approx Z_0$, the reflection coefficient S_{11} tends to zero, which enhances absorption. Effective medium theory (EMT) models a metamaterial as a uniform medium by averaging its microscopic structure to determine effective parameters such as permittivity and permeability. This method aids in understanding and forecasting the overall electromagnetic response of intricate metamaterial designs. From S-parameters (reflection S_{11}, transmission S_{21}), effective parameters can be extracted using retrieval techniques like Nicolson–Ross–Weir (NRW).

$$\eta = \frac{1}{kd} \cos^{-1}\left[\frac{1-S_{11}^2+S_{21}^2}{2S_{21}}\right] \quad (2)$$

Where η is the refractive index and d is the thickness.

2.2. Absorber design and simulation setup

A set of three metal-dielectric-metal MMA layers is proposed in Figure 1. The MMA patch and grounded layer were designed using copper. For comparison, the dielectric substrate material used in this contribution was FR4 material (ε_r=4.3, tan δ=0.025). The unit cell patch is designed based on four complementary squares with embedded phi and T arms. The substrate material of interest is 8.6×8.6×1.6 mm³ in physical dimension, and its copper layer is 0.035 mm thick. Where L_1=4 mm, w_1=4 mm, t=0.5 mm, g=0.4 mm, g_1=0.2 mm, L_2=3.3 mm, W_2=3.3 mm, L_3=2.6 mm, W_3=2.6 mm, L_4=1.9 mm, W_4=1.9 mm, L_5=2.4

mm, W_5=1.2 mm and g_2=0.25 mm. The unit cell is positioned between positive and negative waveguide port directions, with PEC and PMC boundaries applied along the X- and Y-axes, respectively. The MMA design uses scattering parameters and a surface-based tetrahedral meshing approach. A schematic illustration of the proposed metamaterial unit cell structure shown in Figure 1(a) and its boundary conditions and wave ports is shown in Figure 1(b).

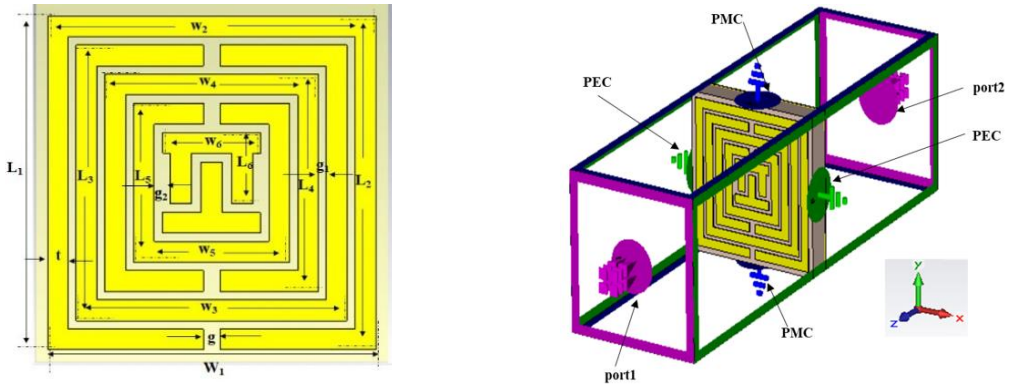

(a) (b)

Figure 1. Three-layer metamaterial absorber configuration for 5G application (a) front view with different dimensions and (b) simulation setup with boundary conditions

A frequency domain solver with 1,001 samples from 2–9 GHz was employed with the parameters shown in Figure 2. The S-parameters are shown in Figure 2(a). Initially tested in CST, the final simulations were conducted in high-frequency structure simulator (HFSS), which uses finite element method (FEM), unlike CST's finite integration technique (FIT). As shown in Figure 2(b), S_{11} values from both tools are closely matched: CST and HFSS show −10.64 dB at 3.554 GHz and −10.66 dB at 3.414 GHz, respectively. HFSS records −22.27 dB at 4.835 GHz, while CST gives −30.27 dB at 4.940 GHz. At higher frequencies, CST shows −13.95 dB at 8.335 GHz and HFSS −16.80 dB at 8.314 GHz. These close correlations confirm that both simulation platforms validate the unit cell design effectively.

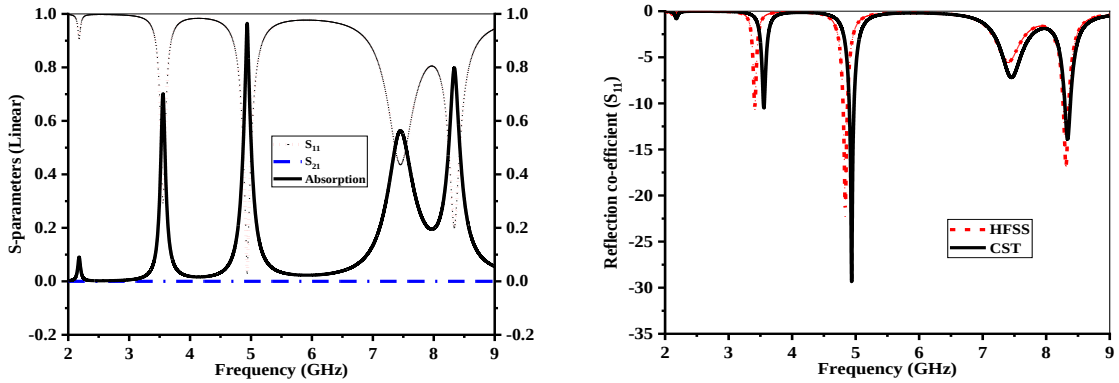

(a) (b)

Figure 2. The EM performance of the proposed design (a) simulated S-parameters and (b) S11 obtained from CST and HFSS

The absorption characteristic of the proposed MMA is determined via (3) as mentioned [22].

$$A = 1 - S_{11}^2 - S_{21}^2 \quad (3)$$

Where S_{21} is the transmission coefficient and S_{11} is the reflection coefficient. The conductivity of the copper ground: σ=5.8×107 S/m, and the ground is also copper. The other parameters applied to the project are for the copper, generally used for electrical and electronic applications, the skin depth of the electromagnetic wave is 0.0105 millimeters. Then it makes perfect sense to assume the EM wave would be obstructed in the 0.035 mm-thick ground layer, so S_{21}=0. Thus, express the absorption as (4).

$$A = 1 - S_{11}^2 \quad (4)$$

2.3. Absorber design procedure

The design step and their corresponding absorption is shown in Figure 3. The final design is achieved through a series of structural modifications. Design 1 and Design 2 both include a pie-shaped element combined with a split square ring, while Design 2 also incorporates an inverted T-shape. To develop the final design, the pie and inverted T elements were combined, and multiple split square rings were added incrementally, as illustrated in Figure 3(a). The absorption characteristics of the various design stages are shown in Figure 3(b). Design 1 attains a maximum absorption of 56% with a single resonance point at 6.690 GHz. Design 2, with a single resonance at 7.271 GHz, reached 74.07%, and Design 3, with a single resonance at 6.858 GHz, reached 57.98%. The absorption efficiency increases as the designs advance. With two resonance points, designs 4 and 5 exhibit higher absorption rates, 84.64% at 7.740 GHz achieves 78.62% at 5.045 GHz. The highest absorption rate of 96.94% is shown by the final design, which has three resonance points at 3.554 GHz, 4.940 GHz, and 8.335 GHz with absorption 70.63%, 96.94%, and 79.93%, respectively.

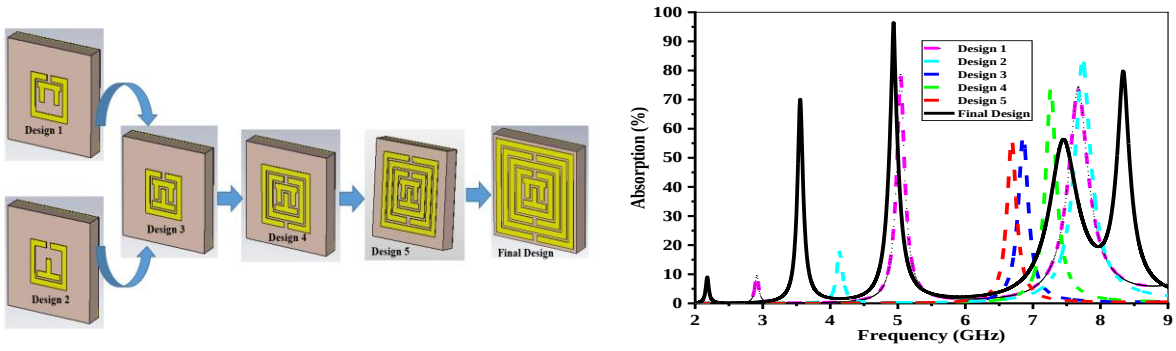

Figure 3. Evaluation of the (a) design structure and (b) absorption in metamaterial absorber for 5G application

3. RESULTS ANALYSIS AND DISCUSSION

3.1. Parametric results

This section presents a parametric study analyzing the impact of substrate material and thickness on absorber performance. The results underscore the importance of selecting optimal substrate properties to enhance absorption and achieve peak performance across target frequency ranges.

3.1.1. Effect of substrate materials and thickness

The effect of substrate materials and substrate thickness on absorption was analyzed, considering their electrical and mechanical properties shown in Figure 4. As shown in Figure 4(a), FR-4 delivered the best performance with 96.94% absorption at 4.940 GHz and three resonance points. Rogers RT5880 performed well at lower frequencies, with 55.16% at 2.784 GHz, while porcelain and quartz showed moderate absorptions of 53.81% at 3.050 GHz and 49.10% at 3.743 GHz, respectively, highlighting the importance of material selection. Substrate thickness was also evaluated at 1.50 mm, 1.60 mm, and 1.70 mm, each showing three resonances. The 1.60 mm thickness achieved the highest absorption of 96.94% at 4.940 GHz, followed by 94.94% at 4.926 GHz (1.70 mm) and 92.39% at 4.954 GHz (1.50 mm), as illustrated in Figure 4(b). Thus, 1.60 mm was identified as the optimal thickness, offering the best balance between peak frequency and absorption. These results emphasize the crucial role of both substrate material and thickness in absorber optimization.

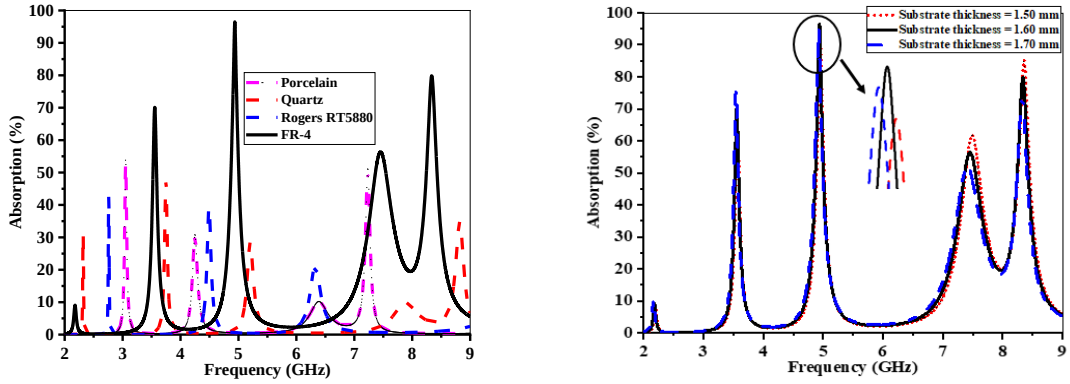

(a) (b)

Figure 4. Absorption for different (a) substrate materials and (b) substrate thicknesses

3.1.2. Effect of array structures and structural dimensions

The impact of array configurations and size on absorber performance was systematically examined in Figure 5. Each topology influenced resonance and wave interactions due to unique geometries. As shown in Figure 5(a), the compact 1:2 array yielded the highest absorption of 97.06% at 4.894 GHz with four resonances centered at 4.898 GHz. The 2:2 and 3:3 arrays also performed well, peaking at 95.82% (4.842 GHz) and 94.00% (4.723 GHz), respectively, confirming design robustness. The effect of physical dimensions was also assessed, revealing a trade-off between size and performance. Larger absorbers offered broader bandwidth but are less suitable for compact systems, while smaller ones, though more efficient at target frequencies, may suffer bandwidth reduction and impedance mismatch. As seen in Figure 5(b), the 8.6 mm×8.6 mm design achieved 96.94% absorption at 4.940 GHz, outperforming the 8 mm×8 mm (74.52% at 4.737 GHz) and 9.2 mm×9.2 mm (93.74% at 5.038 GHz) configurations. These results highlight the need to balance size and performance based on application needs.

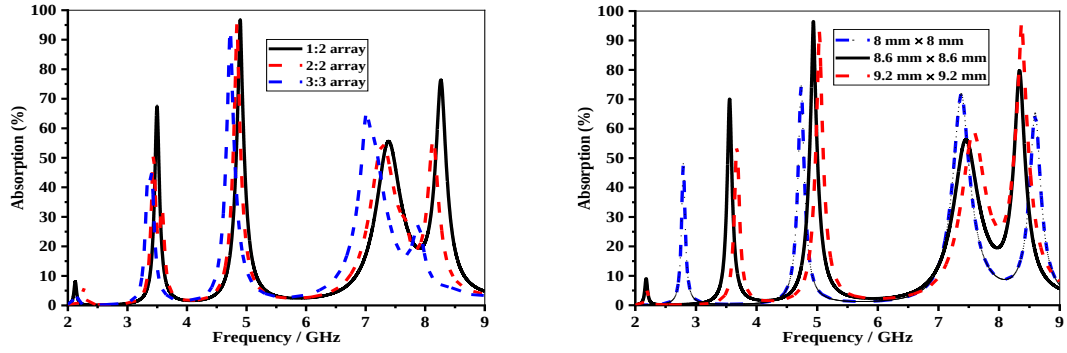

(a) (b)

Figure 5. Absorption analysis for various (a) arrays and (b) structural dimensions

3.2. Electric field, magnetic field, surface current, and power flow

The absorption behavior is clarified through surface current, E-field, H-field, and power flow analysis shown in Figure 6. At 4.94 GHz shown in Figure 6(a), the inner ring current circulates clockwise, while the outer ring segments show mixed current orientations. The left, upper, and lower outer segments exhibit anticlockwise current flow, whereas the right-side segments (both upper and lower) circulate clockwise. This creates an anti-parallel current configuration along the right arm, indicating strong magnetic coupling and field cancellation in that region. The relationship between the surface distributions of current, electric field, and magnetic field can be explored through Maxwell's (5) and (6) [23], [24]. In (5) represents Faraday's law of electromagnetic induction, while (6) corresponds to the modified Ampere's law, involving the displacement current term $\partial D/\partial t$. We can see the relation between the E and H vectors in (7) and (8).

$$\nabla \times E = -\partial B/\partial t \quad (5)$$

$$\nabla \times H = J + \partial D/\partial t \quad (6)$$

$$D(t) = \varepsilon(t) \times E(t) \quad (7)$$

$$B(t) = \mu(t) \times H(t) \quad (8)$$

The electric flux density is denoted by D, ε, and μ represent the permittivity and permeability, respectively. By considering the time dependence $e^{-j\omega t}$ and substituting the time derivative jω into (9) and (10), Maxwell's equations can be rewritten as.

$$\nabla \times E = -j\omega\mu H \quad (9)$$

$$\nabla \times H = j\omega\varepsilon E \quad (10)$$

In Figure 6(b) at 4.94 GHz, the electric field (E-field) is strongly concentrated along the inner and outer ring edges, especially at the gaps, indicating intense capacitive coupling. The high field regions (in red) suggest strong resonance and energy confinement within the metamaterial structure. So the absorption at this frequency is highest (96.936%). The magnetic field intensity showed in Figure 6(c) is mainly concentrated in the central region of the structure, with stronger values (red) extending upward and weaker fields (green to blue) near the bottom. This gradient distribution indicates a strong magnetic dipole formation along the vertical axis. The field confinement near the center suggests efficient magnetic resonance at 4.94 GHz. Power loss analysis in Figure 6(d) shows absorption is dominated by resonator structures, with metallic losses prevailing at sub-GHz due to FR-4's $\tan\delta = 0.025$. These combined field interactions validate the triple-resonance absorption behavior across the observed frequencies.

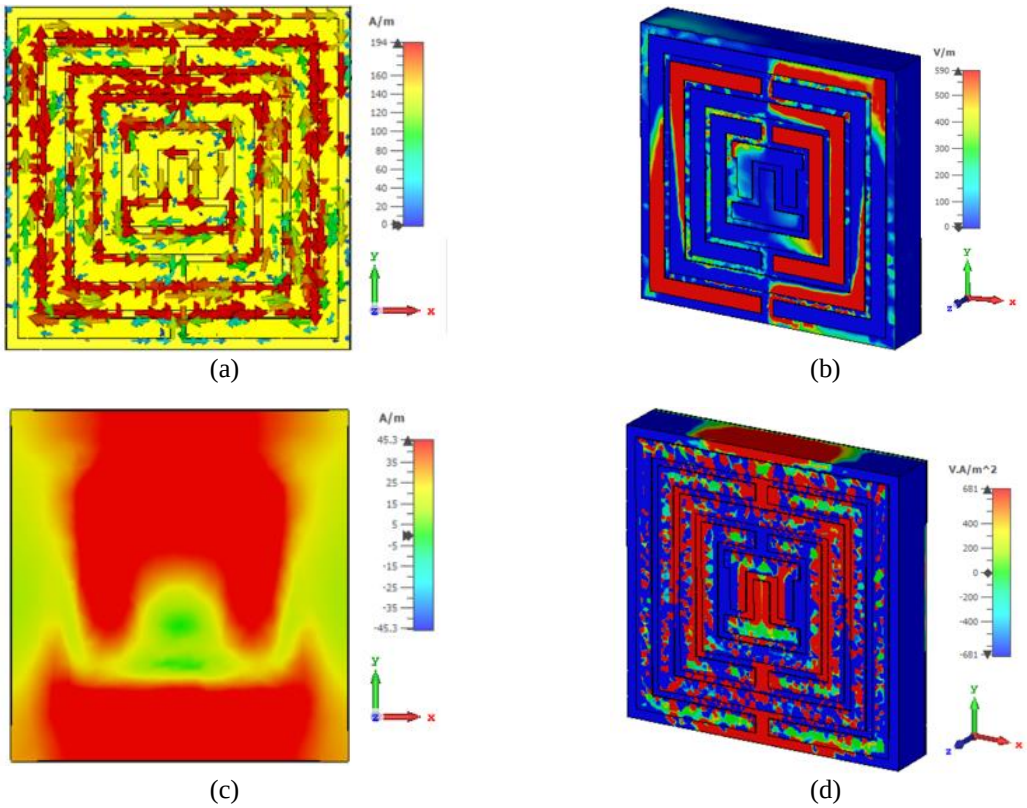

Figure 6. The analysis of: (a) surface current flow, (b) electric field distribution, (c) magnetic field distribution, and (d) power flow at resonance frequency 4.94 GHz

Multiple comparison is shown in Table 1 with the proposed absorber. The proposed metamaterial absorber exhibits superior compactness, with dimensions of 8.6×8.6×1.6 mm³, which is significantly smaller than most referenced designs, while maintaining a high peak absorption of 96.94% at 4.94 GHz. Using a low-cost FR-4 substrate, it achieves the highest EMR of 9.83, indicating excellent miniaturization without compromising performance. Compared to other absorbers with larger sizes and similar or lower absorption

rates, this design effectively balances size, absorption efficiency, and substrate cost, making it a promising candidate for practical 5G applications. Future work may involve tunable materials and conformal applications to expand utility. Overall, the MMA is a viable, low-cost solution for advanced 5G system integration.

Table 1. Comparison among previous configurations and proposed configurations

Reference	Dimension (mm^3)	Substrate material	Peak frequency (GHz)	Peak absorption (%)	EMR
[3]	40×20×6.25	PET-PDMS-PET	3.2-11	80.00%	2.34
[6]	40×40×11	PET-PDMS-PET	2.2-5.83	80.00%	3.40
[12]	33.5 × 33.5 × 6	Neoprene rubber	1.75	96.91%	5.11
[14]	13.8 × 13.8 × 1	FR-4	4.4, 6.05, 13.9	97.00%	4.94
[25]	10 × 10 × 0.8	FR-4	5.92	94.50%	7.59
[26]	32.4 × 34 × 0.1	PET	1-4.5	90.00%	8.82
Proposed	8.6 × 8.6 × 1.6	FR-4	4.940	96.94%	9.83

4. CONCLUSION

This paper proposes a new miniaturized metamaterial absorber MMA with ultra-thin thickness, EMR 9.83, using the well-known MSSRR. Since MMA can be used for 5G applications in the sub-7 GHz and sub-8 GHz frequency range, the MMA exhibits high absorption efficiency corresponding with the resonance frequencies 70.63% at 3.554 GHz, 96.94% at 4.940 GHz, and 79.93% at 8.335 GHz. Its small dimension and design on an FR-4 substrate also make it more applicable in real life. The simulation results of CST and HFSS software are matched well, which demonstrates that the MMA is viable to absorb the signal and decrease the SAR. Therefore, the proposed MMA offers a high-performance, low-cost, and compact solution for integration into modern 5G systems with promising scope for further enhancement and practical deployment.

ACKNOWLEDGMENTS

Sincere thanks to CASR, DUET officials, and the Vice-Chancellor for supporting and endorsing this research.

FUNDING INFORMATION

This study is funded by the Vice-Chancellor's Research Fund, DUET, Gazipur.

AUTHOR CONTRIBUTIONS STATEMENT

This journal uses the Contributor Roles Taxonomy (CRediT) to recognize individual author contributions, reduce authorship disputes, and facilitate collaboration.

Name of Author	C	M	So	Va	Fo	I	R	D	O	E	Vi	Su	P	Fu
Mohammad Jakir Hossain	✓	✓	✓	✓	✓	✓		✓	✓	✓			✓	
Md. Alim Uddin		✓	✓	✓		✓		✓	✓	✓	✓	✓		✓
Md. Mesbahul Islam	✓		✓				✓			✓			✓	✓
Keya Ghosh		✓	✓	✓		✓		✓	✓	✓	✓			
Nusrat Jahan	✓		✓				✓			✓			✓	✓
Mukta Akter Asma		✓	✓		✓		✓		✓			✓		

C : **C**onceptualization
M : **M**ethodology
So : **So**ftware
Va : **Va**lidation
Fo : **Fo**rmal analysis
I : **I**nvestigation
R : **R**esources
D : **D**ata Curation
O : Writing - **O**riginal Draft
E : Writing - Review & **E**diting
Vi : **Vi**sualization
Su : **Su**pervision
P : **P**roject administration
Fu : **Fu**nding acquisition

CONFLICT OF INTEREST STATEMENT

No conflict of interest.

DATA AVAILABILITY

Data availability is not applicable to this paper as no new data were created or analyzed in this study.

REFERENCES

[1] J. Khan *et al.*, "Design and performance comparison of rotated Y-shaped antenna using different metamaterial surfaces for 5G mobile devices," *Computers, Materials & Continua*, vol. 60, no. 2, pp. 409–420, 2019, doi: 10.32604/cmc.2019.06883.

[2] A. Tikhomirov, E. Omelyanchuk, and A. Semenova, "Recommended 5G frequency bands evaluation," in *2018 Systems of Signals Generating and Processing in the Field of on Board Communications*, Mar. 2018, pp. 1–5, doi: 10.1109/sosg.2018.8350639.

[3] Y. Wu, J. Wang, S. Lai, X. Zhu, and W. Gu, "Transparent and flexible broadband absorber for the sub-6G band of 5G mobile communication," *Optical Materials Express*, vol. 8, no. 11, p. 3351, Oct. 2018, doi: 10.1364/ome.8.003351.

[4] Huawei, "5G spectrum." https://www.huawei.com/en/public-policy/5g-spectrum (accessed Apr. 30, 2023).

[5] C. Guan *et al.*, "Broadband tunable metasurface platform enabled by dynamic phase compensation," *Optics Letters*, vol. 47, no. 3, p. 573, Jan. 2022, doi: 10.1364/ol.449863.

[6] Y. Wu, J. Wang, S. Lai, X. Zhu, and W. Gu, "A transparent and flexible microwave absorber covering the whole WiFi waveband," *AIP Advances*, vol. 9, no. 2, Feb. 2019, doi: 10.1063/1.5083102.

[7] X. Chen, W. Li, Z. Wu, Z. Zhang, and Y. Zou, "Origami-based microwave absorber with a reconfigurable bandwidth," *Optics Letters*, vol. 46, no. 6, p. 1349, Mar. 2021, doi: 10.1364/ol.419093.

[8] Q. Wang and Y. Cheng, "Compact and low-frequency broadband microwave metamaterial absorber based on meander wire structure loaded resistors," *AEU - International Journal of Electronics and Communications*, vol. 120, p. 153198, Jun. 2020, doi: 10.1016/j.aeue.2020.153198.

[9] Y. Cheng, H. Luo, and F. Chen, "Broadband metamaterial microwave absorber based on asymmetric sectional resonator structures," *Journal of Applied Physics*, vol. 127, no. 21, Jun. 2020, doi: 10.1063/5.0002931.

[10] P. Jain *et al.*, "An ultrathin compact polarization-sensitive triple-band microwave metamaterial absorber," *Journal of Electronic Materials*, vol. 50, no. 3, pp. 1506–1513, Jan. 2021, doi: 10.1007/s11664-020-08680-z.

[11] W. Li, J. Wei, W. Wang, D. Hu, Y. Li, and J. Guan, "Ferrite-based metamaterial microwave absorber with absorption frequency magnetically tunable in a wide range," *Materials & Design*, vol. 110, pp.27-34, Nov. 2016, doi: 10.1016/j.matdes.2016.07.118.

[12] K. P. Kaur, T. Upadhyaya, M. Palandoken, and C. Gocen, "Ultrathin dual-layer triple-band flexible microwave metamaterial absorber for energy harvesting applications," *International Journal of RF and Microwave Computer-Aided Engineering*, vol. 29, no. 1, p. e21646, Jan. 2019, doi: 10.1002/mmce.21646.

[13] A. K. Singh, M. P. Abegaonkar, and S. K. Koul, "A triple band polarization insensitive ultrathin metamaterial absorber for S-C- and X-bands," *Progress In Electromagnetics Research M*, vol. 77, pp. 187–194, 2019, doi: 10.2528/pierm18110601.

[14] X. Zeng, M. Gao, L. Zhang, G. Wan, and B. Hu, "Design of a triple-band metamaterial absorber using equivalent circuit model and interference theory," *Microwave and Optical Technology Letters*, vol. 60, no. 7, pp. 1676–1681, May 2018, doi: 10.1002/mop.31219.

[15] F. Ö. Alkurt *et al.*, "Design of a dual band metamaterial absorber for Wi-Fi bands," in *AIP Conference Proceedings*, 2018, vol. 1935, p. 060001, doi: 10.1063/1.5025979.

[16] F. Tofigh, M. Amiri, N. Shariati, J. Lipman, and M. Abolhasan, "Polarization-insensitive metamaterial absorber for crowd estimation based on electromagnetic energy measurements," *IEEE Transactions on Antennas and Propagation*, vol. 68, no. 3, pp. 1458–1467, Mar. 2020, doi: 10.1109/tap.2019.2955275.

[17] M. Moniruzzaman, M.T. Islam, G. Muhammad, M.S.J. Singh, and M. Samsuzzaman, "Quad band metamaterial absorber based on asymmetric circular split ring resonator for multiband microwave applications," *Results in Physics*, vol. 19, p.103467, Dec. 2020, doi: 10.1016/j.rinp.2020.103467.

[18] S. Hannan, M. T. Islam, M. R. I. Faruque, and H. Rmili, "Polarization-independent perfect metamaterial absorber for C, X and, Ku band applications," *Journal of Materials Research and Technology*, vol. 15, pp. 3722–3732, Nov. 2021, doi: 10.1016/j.jmrt.2021.10.007.

[19] T. Ramachandran, M. R. I. Faruque, A. M. Siddiky, and M. T. Islam, "Reduction of 5G cellular network radiation in wireless mobile phone using an asymmetric square shaped passive metamaterial design," *Scientific Reports*, vol. 11, no. 1, Jan. 2021, doi: 10.1038/s41598-021-82105-7.

[20] Y. Cheng, Y. Zou, H. Luo, F. Chen, and X. Mao, "Compact ultra-thin seven-band microwave metamaterial absorber based on a single resonator structure," *Journal of Electronic Materials*, vol. 48, no. 6, pp. 3939–3946, Mar. 2019, doi: 10.1007/s11664-019-07156-z.

[21] H. Luo and Y. Z. Cheng, "Ultra-thin dual-band polarization-insensitive and wide-angle perfect metamaterial absorber based on a single circular sector resonator structure," *Journal of Electronic Materials*, vol. 47, no. 1, Sep. 2017, doi: 10.1007/s11664-017-5770-8.

[22] Y. Cheng, F. Chen, and H. Luo, "Plasmonic chiral metasurface absorber based on bilayer fourfold twisted semicircle nanostructure at optical frequency," *Nanoscale Research Letters*, vol. 16, no. 1, Jan. 2021, doi: 10.1186/s11671-021-03474-6.

[23] M. S. Wartak, K. L. Tsakmakidis, and O. Hess, "Introduction to metamaterials," *Physics in Canada*, vol. 67, pp. 30–34, 2011.

[24] M. L. Hakim *et al.*, "Wide-oblique-incident-angle stable polarization-insensitive ultra-wideband metamaterial perfect absorber for visible optical wavelength applications," *Materials*, vol. 15, no. 6, p. 2201, Mar. 2022, doi: 10.3390/ma15062201.

[25] D. Sood, "Ultrathin compact triple-band polarization-insensitive metamaterial microwave absorber," in *Mobile Radio Communications and 5G Networks*, Springer Singapore, 2020, pp. 607–617.

[26] D. Zha *et al.*, "A multimode, broadband and all-inkjet-printed absorber using characteristic mode analysis," *Optics Express*, vol. 28, no. 6, p. 8609, Mar. 2020, doi: 10.1364/oe.384954.

BIOGRAPHIES OF AUTHORS

Mohammad Jakir Hossain was awarded doctor of engineering in space science from the Universiti Kebangsaan Malaysia (UKM), Malaysia. He joined the Department of Electrical and Electronic Engineering (EEE) of Dhaka University of Engineering and Technology (DUET), Gazipur, in 2006. He has currently serving as a professor of the Department of EEE at DUET, since 2020. His research interests include metamaterials, metamaterial-based absorbers, antennas, wireless communication, microwaves, and satellite communication. Furthermore, he is a life fellow of the Institution of Engineers, Bangladesh (IEB). He can be contacted at email: jakir@duet.ac.bd.

Md. Alim Uddin is a postgraduate student in electrical and electronic engineering at Dhaka University of Engineering and Technology (DUET), Gazipur. Born in Kushtia, Bangladesh, in 2000, he is actively involved in academic research. He has authored two refereed journal articles and two conference papers. His primary research interests include metamaterials and metamaterial-based absorbers, antenna, microwave devices, and satellite communication. Recently, he has expanded his focus to quantum materials and quantum sensors. He can be contacted at email: abdulalim156686@gmail.com.

Md. Mesbahul Islam was born in Joypurhat, Bangladesh, in 1998. He is an undergraduate (UG) student in the Department of Electrical and Electronic Engineering, Dhaka University of Engineering and Technology, Gazipur. He has participated in multiple international research work. His main research focuses on metamaterials and absorbers based on metamaterial structures. Additionally, he is involved in antenna design and microwave engineering. He can be contacted at email: mesbaulislam23@gmail.com.

Keya Ghosh was born in Narail, Bangladesh, in 1995. She has completed her bachelor of science (B.Sc.) in engineering from the Department of Electrical and Electronic Engineering at Dhaka University of Engineering and Technology (DUET), Gazipur. Currently, she is pursuing her master of science (M.Sc.) degree in the same department at DUET. Her research interests include metamaterials, metamaterial-based absorbers, and antennas. She can be contacted at email: keyaghosh.nesco@gmail.com.

Nusrat Jahan was born in Gazipur, Bangladesh, in 1998. She has completed her undergraduate (UG) studies in the Department of Electrical and Electronic Engineering at Jatiya Kabi Kazi Nazrul Islam University. Currently, she is pursuing her postgraduate (PG) degree in the same department at Dhaka University of Engineering and Technology, Gazipur. Her research interests include metamaterials, metamaterial-based absorbers, antennas, and wireless communication. She can be contacted at email: nusratjahan17102903@gmail.com.

Mukta Akter Asma was born in Chandpur, Bangladesh, in 2000. She is a undergraduate (UG) student in the Department of Electrical and Electronic Engineering, Dhaka University of Engineering and Technology, Gazipur. Her research interests include metamaterials, metamaterial-based absorbers, antennas, IoT, wireless communication, microwaves, and satellite communication. She can be contacted at email: asmaulhousnamukta19623@gmail.com.